

DiffuseTrace: A Transparent and Flexible Watermarking Scheme for Latent Diffusion Model

Liangqi Lei

1120202296@bit.edu.cn

Beijing Institute of Technology
Beijing, China

Jing Yu

yujing02@iie.ac.cn

Institute of Information Engineering, CAS
Beijing, China

Keke Gai

gaikeke@bit.edu.cn

Beijing Institute of Technology
Beijing, China

Liehuang Zhu

liehuangz@bit.edu.cn

Beijing Institute of Technology
Beijing, China

ABSTRACT

Latent Diffusion Models (LDMs) enable a wide range of applications but raise ethical concerns regarding illegal utilization. Adding watermarks to generative model outputs is a vital technique employed for copyright tracking and mitigating potential risks associated with AI-generated content. However, post-hoc watermarking techniques are susceptible to evasion. Existing watermarking methods for LDMs can only embed fixed messages. Watermark message alteration requires model retraining. The stability of the watermark is influenced by model updates and iterations. Furthermore, the current reconstruction-based watermark removal techniques utilizing variational autoencoders (VAE) and diffusion models have the capability to remove a significant portion of watermarks. Therefore, we propose a novel technique called DiffuseTrace. The goal is to embed invisible watermarks semantically in all generated images for future detection. The method establishes a unified representation of the initial latent variables and the watermark information through training an encoder-decoder model. The watermark information is embedded into the initial latent variables through the encoder and integrated into the sampling process. The watermark information is extracted by reversing the diffusion process and utilizing the decoder. DiffuseTrace does not rely on fine-tuning of the diffusion model components. The watermark is embedded into the image space semantically without compromising image quality. The encoder-decoder can be utilized as a plug-in in arbitrary diffusion models. We validate through experiments the effectiveness and flexibility of DiffuseTrace. DiffuseTrace holds an unprecedented advantage in combating the latest attacks based on variational autoencoders and Diffusion Models.

CCS CONCEPTS

• **Security and privacy** → *Security services.*

Permission to make digital or hard copies of all or part of this work for personal or classroom use is granted without fee provided that copies are not made or distributed for profit or commercial advantage and that copies bear this notice and the full citation on the first page. Copyrights for components of this work owned by others than the author(s) must be honored. Abstracting with credit is permitted. To copy otherwise, or republish, to post on servers or to redistribute to lists, requires prior specific permission and/or a fee. Request permissions from permissions@acm.org.

Conference acronym 'XX, June 03–05, 2024, Woodstock, NY

© 2024 Copyright held by the owner/author(s). Publication rights licensed to ACM.

ACM ISBN 978-1-4503-XXXX-X/18/06...\$15.00

<https://doi.org/XXXXXXX.XXXXXXX>

KEYWORDS

Latent Diffusion Model, Model Watermarking, Copyright Protection, Security

ACM Reference Format:

Liangqi Lei, Keke Gai, Jing Yu, and Liehuang Zhu. 2024. DiffuseTrace: A Transparent and Flexible Watermarking Scheme for Latent Diffusion Model. In *Proceedings of Make sure to enter the correct conference title from your rights confirmation email (Conference acronym 'XX)*. ACM, New York, NY, USA, 14 pages. <https://doi.org/XXXXXXX.XXXXXXX>

1 INTRODUCTION

The strides made in latent diffusion models [10, 17, 28, 35] have substantially elevated the capacity for synthesizing photorealistic content in image generation and profoundly impact text-to-image [32, 46], image editing [5, 24], in-painting [21, 31], super-resolution [12, 33], content creation [26, 27] and video synthesis [4, 16]. Relevant applications are becoming mainstream creative tools for designers, artists, and the general public.

However, contemporary text-to-image generation models, such as Stable Diffusion and Midjourney, can generate a multitude of novel images as well as convincing depictions of fabricated events for malicious purposes. Criminals might utilize LDMs to produce insulting or offensive images, which shall be disseminated to spread rumors and pose a substantial threat to societal security. The hazards of deepfakes, impersonation and copyright infringement are also prevalent issues associated with current generative models.

The potential illicit use of text-to-image models has spurred research for embedding watermarks in model outputs. Watermarked images contain signals imperceptible to humans but are marked as machine-generated. Copyright information of the model and the identity information of the model users will be embedded into images. Extracting watermarks from AI-generated images enables the detection of model copyrights and tracing unauthorized users. False and harmful images can be promptly identified and removed from platforms and unauthorized users of the model can be traced through the extraction of image information, which mitigates the potential harm caused by AI-generated content.

Existing research on image watermarking tended towards post-processing solutions. The core concept involves embedding the watermark into the image with minimal adjustments, emphasizing subtlety and intricacy. For instance, the watermark implemented

in Stable Diffusion [8] operates by altering a particular Fourier frequency within the generated image. This type of watermark faces a key trade-off between watermark robustness and image quality. For diffusion model watermarks, Some researchers have proposed embedding fixed messages into generated images by fine-tuning diffusion models like U-Net [30] or variational autoencoders. However, this approach only allows embedding fixed information into the generated images, requiring re-finetuning of the diffusion model when the embedding information needs to be changed. Moreover, if the model owner distributes the diffusion model to a large number of users, each distributed model must be fine-tuned separately, resulting in significant consumption of computational resources and time. Additionally, when the model requires iterative updates, the stability of the watermark becomes unreliable due to adjustments in model parameters. Recent studies [48] have demonstrated that methods involving the random addition of noise to images to disrupt watermarks, followed by image reconstruction using diffusion models, can effectively remove a significant portion of post-processing watermarking schemes. This poses new challenges to the robustness of watermarking.

To address the aforementioned challenges and achieve high extraction accuracy, robustness and image quality, we propose a new watermarking scheme called DiffuseTrace. DiffuseTrace differs fundamentally from previous watermarking methods. DiffuseTrace embeds the watermark into the latent variables of the model, subtly influencing the sampling phase of the model. The watermark is embedded at the semantic level prior to image generation, without any post-processing of the generated images. We specialize in a watermarking scheme that can be seamlessly integrated into a wide range of latent diffusion models. DiffuseTrace can serve as a plug-and-play solution across various diffusion models.

Taking practical application scenarios into account, we categorize the roles involved in model usage into two types: model producers and model users. Model producers train and possess all pre-trained models, including diffusion models, watermark encoders, watermark decoders. Model producers assign specific binary identity information to each user. By providing APIs, model producers offer generative model services to users. When malicious images resembling model-generated content or images suspected of copyright infringement appear on art platforms, news outlets or other sharing platforms, model producers can trace illegal usage or infringement-involved users by extracting watermark information from the generated images.

For watermark modules, we control the distribution of the watermark through an encoder and dynamically allocate a watermark close to the standard normal distribution for each user. Since the data distribution and sampling process remain consistent with the original model, the generated images can achieve transparent watermark embedding with semantic consistency. Human inspection cannot distinguish watermark samples from random samples. Through transforming images into latent variables and inversely diffusing them to obtain the initial latent variables, the watermark can be decoded through a decoder. Considering the diverse processing stages in the flow of image data as well as the potential bias introduced by the inverse diffusion of the diffusion model, we employ adversarial training and fine-tuned the watermark decoder to enhance the robustness of watermark extraction.

The primary contributions of this work are outlined as follows:

- (1) Among diffusion watermarking schemes based on initial hidden variables, DiffuseTrace is the first scheme that embeds robust multi-bit watermarks. DiffuseTrace is embedded at the semantic level of diffusion-model-generated images without relying on the trade-off between image quality and watermark robustness. It exhibits evident advantages over post-processing methods in terms of image quality.
- (2) Compared to the state-of-the-art post-processing watermarking and diffusion model watermarking schemes, DiffuseTrace not only exhibits significant performance in common image processing but also shows remarkable robustness against attacks based on variational autoencoders and diffusion models. The paper provides a thorough analysis at the theoretical level regarding the superior watermark robustness of DiffuseTrace.
- (3) The proposed universal watermark module for latent diffusion models can be seamlessly integrated across different versions of diffusion models. The watermark message of DiffuseTrace can be flexibly modified without being affected by model fine-tuning or model update iterations. Our code is open source: <https://anonymous.4open.science/r/DiffuseTrace-6DED>.

Paper Organization. The overview of this paper is organized as follows: The basic introduction of DiffuseTrace is shown in Section 1. The background of DiffuseTrace are summarized in Section 2. In Section 3, we introduce the problem formulation for DiffuseTrace. In Section 4, we demonstrate DiffuseTrace in detail. In Section 5, We have provided a detailed theoretical exposition and security analysis of the proposed scheme. In Section 6, we summarize and analyze the experimental results. In Section 7, we present the realted work of watermarking for LDMs. In Section 8, we summarize the DiffuseTrace watermarking scheme.

2 BACKGROUND

2.1 Diffusion Model based Image Generation

Diffusion models progressively transitions the sample x from the true data distribution $p(x)$ to stochastic noise and adeptly reverses this process through iterative denoising of the noisy data [17]. A typical diffusion model framework involves a forward process that progressively diffuses the data distribution $p(x, c)$ towards the noise distribution $p_t(z_t, c)$ for $t \in (0, T]$, where c denotes the conditional context. The conditional gaussian distribution of the diffusion process can be formulated as:

$$p_t(z_t|x) = p_t(z_t|\alpha_t x, \sigma_t^2 I), \quad (1)$$

where $\alpha_t, \sigma_t \in \mathbb{R}^+$. α_t and σ_t are the strengths of signal and noise respectively decided by a noise scheduler. $z_t = \alpha_t x + \sigma_t \epsilon$ is the noisy data. It has been proved that there exists a denoising process with the same marginal distribution as the forward process [35]. The estimation of the only variable can be derived as:

$$\nabla_{z_t} \log p_t(z_t, c) \approx \frac{\alpha_t x_\theta^t(z_t, c) - z_t}{\sigma_t^2}. \quad (2)$$

Specifically, given a noise-predicting diffusion model parameterized by θ , which is typically structured as a U-Net [30], training can be

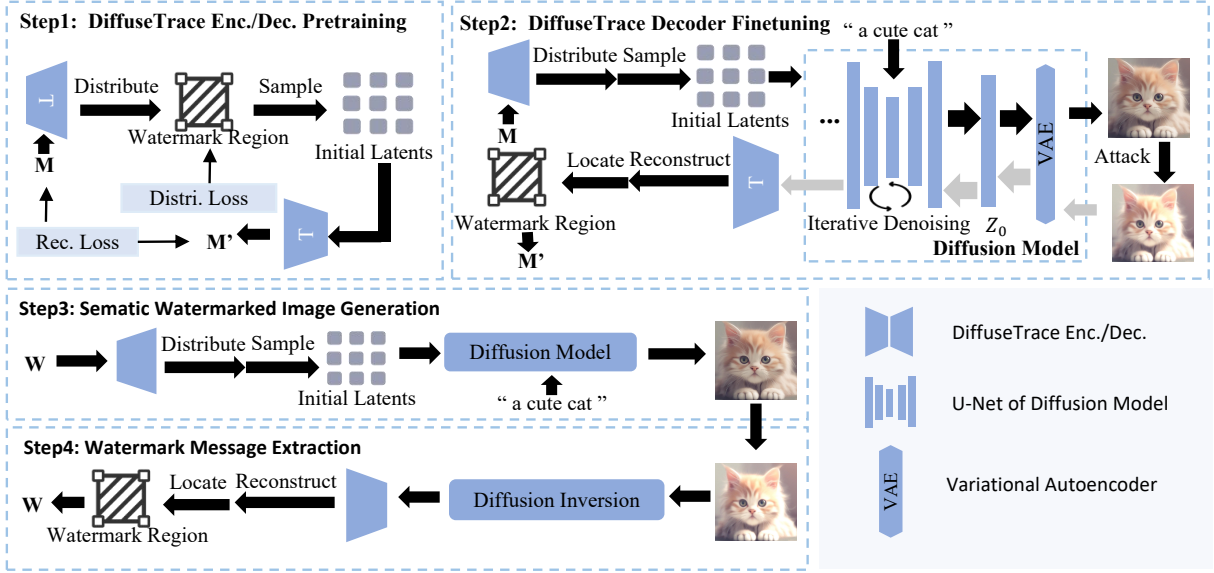


Figure 1: Methods of DiffuseTrace. (Step1) Train the DiffuseTrace Encoder through resampling methods to generate latent variables approximate to a standard normal distribution and jointly train the decoder to decode the information. M : Random n -bit messages. (Step2) Keep the encoder fixed and train the decoder. Randomly select prompts for the diffusion model denoising process to generate images. Decode the images after passing through the attack layer to obtain latent variables and execute diffusion inversion to extract the initial latent variables with the initial message to build a reconstruction loss for fine-tuning the decoder. (Step3) Assign watermark message w and generate initial watermarked latent variables by the encoder to generate images. (Step4) Extract watermark message after inverting the images and trace the source through statistical testing.

formulated as the following noise prediction problem:

$$\min_{\theta} \mathbb{E}_{x,t,\sigma} \|\hat{\epsilon}_{\theta}(\alpha_t x + \sigma_t \epsilon, t) - \epsilon\|_2^2, \quad (3)$$

where t refers to the time step; ϵ is the ground-truth noise; the noise $\epsilon \sim \mathcal{N}(\epsilon|0, I)$ is a standard Gaussian. Recently, LDMs [28] streamlines inference processes by incorporating denoising process within the encoded latent space derived from a pre-trained variational autoencoder (VAE) [6]. Diffusion models reconstructs images through the latent state.

During the inference phase, stable diffusion models take both a latent seed and a text prompt as an input. The U-Net progressively removes noise from random latent image representations guided by text embeddings. The noise residual from the U-Net is utilized in conjunction with a scheduler algorithm to generate a denoised latent. When synthesizing images, a crucial technique, classifier-free guidance is adopted to enhance the quality of generated images.

$$\tilde{\epsilon}_{\theta}(t, z_t, c) = w \hat{\epsilon}_{\theta}(t, z_t, c) + (w - 1) \hat{\epsilon}_{\theta}(t, z_t, \phi) \quad (4)$$

where The guidance scale w can be modified to regulate the influence of conditional information on the produced images, aiming to strike a balance between quality and diversity. $\hat{\epsilon}_{\theta}(t, z_t, \phi)$ denotes the unconditional diffusion obtained by empty prompt.

2.2 Diffusion Denoising and Inversion

The well-trained diffusion model leverages a diverse range of samplers to generate samples from noise and execute denoising procedures. A notable denoising method is the Denoising Diffusion

Implicit Model (DDIM) [34] which stands out for its efficiency and deterministic output. DDIM accomplishes denoising with significantly fewer steps. The image x_0 will be reproduced with 50 inference steps to the standard 1000-step process. Formally, for each denoising step t , DDIM utilizes a learned noise predictor ϵ_{θ} to estimate the noise $\epsilon_{\theta}(x_t)$ added to x_0 , which leads to the estimation of x_0 as follows:

$$\hat{x}_0 = \frac{x_t - \sqrt{1 - \bar{\alpha}_t} \epsilon_{\theta}(x_t)}{\sqrt{\bar{\alpha}_t}}. \quad (5)$$

the estimated noise $\epsilon_{\theta}(x_t)$ is recombined with the approximated \hat{x}_0 to compute x_{t-1} :

$$x_{t-1} = \sqrt{\bar{\alpha}_{t-1}} \hat{x}_0 + \sqrt{1 - \bar{\alpha}_{t-1}} \epsilon_{\theta}(x_t). \quad (6)$$

DDIM also incorporates an inversion mechanism [10], which facilitates the reconstruction of the noise representation x_T from an image x_0 . The recovered x_T should be mappable to an image approximate to x_0 . Based on the assumption that $x_{t-1} - x_t \approx x_{t+1} - x_t$, The DDIM inversion shall be formulated as:

$$\hat{x}_{t+1} = \sqrt{\bar{\alpha}_{t+1}} x_0 + \sqrt{1 - \bar{\alpha}_{t+1}} \epsilon_{\theta}(x_t) \quad (7)$$

Essentially, this process follows the forward diffusion process as described in Equation 6. Diffusion inversion, even in zero-text inversion within conditional diffusion, can still achieve decent accuracy. Meanwhile, the method is applicable to deterministic sampling methods like DPM++ [20]. Our watermarking scheme leverages this property of diffusion inversion.

3 PROBLEM FORMULATION

3.1 Threat Model

In this paper, we consider two parties: the defender and the adversary. The defender is the owner of the generative model. Latent diffusion model is deployed as an online service. The core objectives are protecting the copyright of the model and tracing the illegal usage through model outputs. Conversely, the adversary's objective is to disrupt the watermark information in the model output and circumvent the copyright protection and tracing mechanisms of the model.

Adversary's Motivation. The adversary's motivation stems from two aspects: Firstly, training a latent diffusion model requires gathering a significant amount of data, expertise in architecture or algorithms and numerous failed experiments, all of which are expensive. As a result, the model parameters are considered proprietary information for businesses. Generative model services are deployed as online services. Adversaries may manipulate images to destroy watermark information and redistribute the outputs of online services to cloud platforms, effectively becoming commercial competitors. Secondly, Attackers may exploit online generative services to generate insulting or offensive images for malicious purposes such as fabricating fake news or spreading rumors and remove watermarks from the images to evade tracing.

Adversary's Background Knowledge. We assume that adversaries can access the victim's latent diffusion model in a black-box manner. Attackers can query the victim's latent diffusion model with data samples and obtain corresponding responses. Specifically, we categorize adversary background knowledge into two dimensions: the architecture of the victim's diffusion model and the watermark removal capability. For the architecture of the diffusion model, we assume adversaries can access it since such information is typically publicly accessible. Regarding watermark removal capability, we assume adversaries can manipulate images using techniques such as Gaussian blur, color jittering and image compression. Meanwhile, we consider adversaries who possess the capability to perform state-of-the-art watermark removal attacks using variational autoencoders and diffusion models.

3.2 Image Watermarking and Verification

Formally, the validation scheme for generative image watermarking in Diffusers is defined as follows:

The generative image watermarking verification scheme is a tuple $\text{Verification} = \langle \text{Trn}, \text{Emb}, \text{Eva}, \text{Vrf} \rangle$ of processes:

A Train process $\text{Trn}(D, \text{Arc}[\cdot], \text{Enc}[\cdot], L) = \{\text{Enc}[W], \text{Dec}[W]\}$, is a fine-tuning or training process that takes training data $D = \{x_d, y_d\}$ as inputs and outputs the models $\text{Enc}[W]$ and $\text{Dec}[W]$ by minimizing a given loss L .

An embedding process $\text{Emb}(\text{prm}, \text{Arc}[\cdot], \text{Enc}[\cdot], \text{Lat}, \text{Sig}) = \text{Pic}[\text{Sig}]$ is an inference process that embeds the signature Sig into latent variables through an encoder and performs inference through the model $\text{Arc}[\cdot]$ to output the watermarked image $\text{Pic}[\text{Sig}]$.

An quality evaluation process $\text{Eval}(\text{Arc}[\cdot], M, \text{Lat}, \epsilon) = \{\text{True}, \text{False}\}$ is to evaluate whether or not the discrepancy is less than a predefined threshold i.e. $|M(\text{Arc}[W, \text{Sig}], \text{Lat}, \text{Enc}[\cdot]) - M| \leq \epsilon$, where $M(\text{Arc}[W, \text{Sig}], \text{Lat}, \text{Enc}[\cdot])$ denotes the image fidelity or

semantic consistency tested against a set of watermarked latents. M is the target generation performance.

A verification process $\text{Eva}(\text{Img}, \text{Sig}, \text{Atk}, \text{Dec}[\cdot], \epsilon) = \{\text{True}, \text{False}\}$ checks whether the expected signature Sig of a given generative image can be successfully verified by Decoder $\text{Dec}[\cdot]$ when facing image attacks.

Watermark Detection. DiffuseTrace embed a k -bit secret message $m \in \{0, 1\}^k$ into the watermark image. The watermark detection algorithm includes an extractor that can extract the hidden signal m' from the watermarked image. It uses statistical testing to set a threshold $\tau \in \{0, 1, 2 \dots k\}$ for the extracted bits. If the number of matching bits $E(m, m') \geq \tau$, the image is marked as watermarked.

Formally, We establish the hypothesis H1: The image pic is generated by DiffuseTrace against the null hypothesis H0: The image is not generated by DiffuseTrace. Under H_0 , we assume that the extracted bits m'_1, m'_2, \dots, m'_k are independent and identically distributed Bernoulli random variables with a probability of 0.5. $E(m, m')$ follows a binomial distribution $B(k, 0.5)$. Type I error (false positive rate (FPR), σ) equals the probability of $E(m, m')$ exceeding τ , derived from the binomial cumulative distribution function. It has a closed form using the regularized incomplete beta function $I_x(a; b)$.

$$\begin{aligned} \epsilon_1(\tau) &= \mathbb{P}(E(m, m') > \tau \mid H_0) = \frac{1}{2^k} \sum_{i=\tau+1}^k \binom{k}{i} \\ &= I_{1/2}(\tau + 1, k - \tau). \end{aligned} \quad (8)$$

If we reject the null hypothesis H_0 with a p-value less than 0.01, we consider the image to be without a watermark. In practice, for a watermark of 48 bits ($k = 48$), at least 34 bits should be extracted to confirm the presence of the watermark. This provides a reasonable balance between detecting genuine watermarks and avoiding false positives.

3.3 Objective for Watermarking

DiffuseTrace should have the following properties:

Robust against Watermarking Attacking: Images with watermarks may undergo various image processing operations. Even after post-processing, the watermark can still be fully recovered. DiffuseTrace should withstand watermark removal attacks, such as Gaussian noise, color jittering, Gaussian blur and others. Meanwhile, DiffuseTrace should be able to defend against the latest watermark attacks based on the state-of-the-art variational autoencoder and diffusion model techniques.

Generalizability: Considering the cost of embedding fixed information into fine-tuned models, DiffuseTrace can adjust embedded message flexibly and should be compatible with various versions of diffusion models and remain unaffected by model fine-tuning or model update iterations.

Fidelity: Minimizing the impact on the model's output before and after watermarking to the greatest extent possible. The images generated by the DiffuseTrace maintain consistency with the original model in terms of semantic consistency and image quality. The watermark samples generated by DiffuseTrace should exhibit no significant differences in visual and semantic quality compared to normal samples.

The goal is to design a watermark that is flexible, robust to post-processing, generalizable and does not compromise the quality or semantic consistency of the image. Additionally, it should remain unaffected by model fine-tuning or update iterations.

4 PROPOSED WATERMARKING SCHEME

4.1 Overview

The overview of our method is in figure 1. As described in the first section, we have three objectives:

- The watermark is embedded into the initial latent variables at the semantic level without altering semantic consistency and image quality.
- Watermark messages can be modified flexibly without re-training or fine-tuning the model.
- The watermark is robust against various image processing techniques and state-of-art watermark removal methods.

The core idea of DiffuseTrace is to embed the watermark into latent variables. The initial latent variables of the latent space are divided into multiple watermark regions, with each region corresponding to a portion of the watermark information. To ensure both lossless quality and semantic consistency of the image, the embedded watermark should approximate a standard normal distribution and be extractable by the decoder.

Specifically, DiffuseTrace consists of a watermark encoder and watermark decoder. The model owner encodes the initial latent variables through the watermark encoder. The latent variables are then processed through a scheduler guided by prompts and denoised through a U-Net. Afterward, latent variables are decoded by a variational autoencoder into watermarked images. The watermarked images are subjected to an attack layer and decoded back into the latent space. Through diffusion inversion, the original latent variables are restored. The watermark is then extracted from the decoded latent variables through the decoder.

4.2 Pre-training Watermark Encoder-Decoder

The paper pretrains the encoder-decoder structure for watermark embedding and extraction. The training objective of the encoder is to construct a unified representation of watermark information and latent variables under a standard Gaussian distribution based on the watermark information and the embedded watermark region. Specifically, when binary identity information of the user is inputted into the encoder, it will produce watermark-embedded latent variables which adhere to a standard Gaussian distribution.

The following explains the reason for latent variables with watermark conforming to a standard normal distribution. When the latent generator of the LDM samples latent variables Z from noise, the function of the U-Net is to iteratively denoise Gaussian noise matrices within the diffusion cycle guided by text and timesteps. By subtracting the predicted noise from random Gaussian noise matrices, the random Gaussian noise matrices are eventually transformed into the latent variables of the image. Since the noise introduced during the training process of the U-Net follows a normal distribution, the initial latent variables of the LDM inference process should ideally approximate a standard normal distribution. When training a variational autoencoder to encode images into latent variables,

one of the training objectives is to approximate the latent variables to adhere roughly to a standard normal distribution. More precisely, the training set for U-net involves repeatedly adding noise from a standard normal distribution to images. With a sufficient number of iterations, the original images will converge close to a standard normal distribution. Hence, during the denoising image generation phase, the initial noise is selected to conform to a standard normal distribution. If there is a significant deviation of the initial noise from the standard normal distribution, it may lead to inconsistencies between image quality and semantics. Watermarked latent variables that are closer to a standard normal distribution better conform to the standard denoising process.

Due to the non-differentiability and gradient descent limitations of distributions, the encoder’s model architecture employs the reparameterization technique to generate watermark-embedded latent variables. Considering the difficulty of explicitly distributing watermark regions at the trillion level, we have adopted an implicit partitioning of the watermark regions. Sampled latent variables are constrained by Kullback-Leibler divergence to approximate a standard normal distribution. Each watermark information independently maps to a portion of the probability distribution. The specific principles are detailed in our theoretical analysis 5. The decoder network is the inverse of the encoder. The training objective of the decoder is to extract watermark information from the initial latent variables. The encoder and decoder are jointly trained to ultimately produce watermark-embedded latent variables that conform to a standard normal distribution. The decoder then outputs the corresponding watermark information based on these latent variables.

According to the analysis of 5.2, the reconstruction of watermark refers to maximizing the expected probability distribution of the watermark w given the latent variable. The loss for reconstructing the message \mathcal{L}_w is calculated as the Mean Square Error (MSE) loss between the original watermark message and the decoded message:

$$\mathcal{L}_w = MSE(message, dec(message')) \quad (9)$$

For the loss of the initial latent variable distribution, We compute the Kullback-Leibler (KL) divergence between the distribution of the latent variables and the standard normal distribution as the distribution loss. KL divergence is a measure of how one probability distribution diverges from the expected probability distribution. Suppose we have two probability distributions P and Q for a random variable ξ . If ξ is a discrete random variable, the KL divergence from P to Q is defined as:

$$\mathbb{D}_{KL}(P||Q) = \sum_i P(i) \ln \left(\frac{P(i)}{Q(i)} \right) \quad (10)$$

According to the analysis of 5.1, we assume that the output follows a normal distribution, denoted as $p_1 \sim \mathcal{N}(\mu_1, \sigma_1^2)$ and the standard normal distribution is denoted as $p_2 \sim \mathcal{N}(0, 1)$. The distribution loss \mathcal{L}_{dist} used in this paper is as follows:

$$\mathcal{L}_{dist} = KL(p_1||p_2) = -\frac{1}{2} \times [2 \log \sigma_1 + 1 - \sigma_1^2 - \mu_1^2] \quad (11)$$

In the above two loss functions, \mathcal{L}_w ensures the correct decoding of watermark information, while \mathcal{L}_{dist} guarantees the initial distribution of latent variables, thereby ensuring the quality and semantic

consistency of the images. The encoder and decoder are jointly trained by minimizing the following loss function:

$$\mathcal{L} = \lambda_1 \mathcal{L}_w + \lambda_2 \mathcal{L}_{dist} \quad (12)$$

λ_1 and λ_2 represent the proportion constant parameter. Therefore, the trained encoder is capable of embedding information into latent variables that approximately adhere to a standard normal distribution, while the decoder can be seen as the inverse process of the encoder to extract the watermark.

4.3 Decoder Fine-Tuning

According to the analysis of 5.3, throughout the entire watermark embedding-extraction process, following factors contribute to decoding imprecision:

- (1) The diffusion inversion process approximates the differences between adjacent step latent variables;
- (2) Since the prompt is not available in the practical scenarios during the decoding stage, we utilize zero-text inversion;
- (3) Potential alterations and manipulations to the image occur through various image processing techniques.

These factors contribute to inevitable deviations in the inferred initial latent variables. In essence, these processes result in a global shift of the initial latent variables in the semantic space of the images. The decoder can accurately extract most of the watermark information, but samples located at the edges of the watermark region exhibit significant inaccuracies. During the fine-tuning phase of the decoder, the objectives are to adapt to the shift occurring in the watermark region and accurately extract the watermark from the attacked samples.

Specifically, we fix the encoder of the watermark model and diffusion model. To simulate the image processing procedures in real-world scenarios, the attack layer employs an image perturbation technique after generating various images with randomly prompted words. The perturbation layer includes randomly adding Gaussian noise, applying Gaussian blur, color jittering and image compression to the images. Adversarial training will enhance the robustness of watermark detectors against image processing.

After inverting the images subjected to image processing, we obtain the modified initial latent variables. We fine-tune the decoder by computing the mean squared error between the decoded messages and the original watermark messages as the loss function.

4.4 Error correction mechanism

The scheme clearly delineates the watermark region, but during watermark detection, the effects of inversion and image processing due to adversarial training on the decoder can lead to overlap in watermark detection areas. This results in bit errors for samples at the edges of the watermark region where overlap occurs during adversarial training. We have provided detailed reasons and explanations in the security analysis 5.4 and elucidated the reasons and necessity for employing error correction codes.

Recursive Systematic Convolutional (RSC) Codes: RSC codes provide a systematic approach to encoding and decoding bitstreams, allowing for error correction of data and adaptive recovery of the original message from corrupted data. Concretely, Given an input bitstream m , the RSC encoder transforms it into another bitstream

$m + c_1 + c_2 \dots c_k$. where each c_i is a bitstream that has the same length as the bitstream m and the symbol $+$ indicates the concatenation of bitstreams. A higher encoding ratio can withstand a greater proportion of errors but results in a lengthier encoded bitstream. When decoding, if the modified bit string $m' + c_1 \dots c_j$ is input to the RSC decoder and the error rate of the encoded stream is less than a certain threshold, the original information m can be recovered. We can utilize this property to make corrections to watermark encoding.

Turbo Codes [3]: Turbo codes can tolerate more bit errors compared to other codes at the same bit rate. A typical Turbo code consists of two convolutional codes and an interleaver. The primary function of the interleaver is to shuffle the outputs of the two convolutional codes, increasing the independence of each code and thus enhancing error correction performance. During the decoding process, an iterative algorithm is utilized to estimate and rectify errors iteratively, thereby enhancing the error correction performance. In our experiments, we utilize Turbo codes as error correction codes to further enhance the stability of watermark extraction.

The specific process involves the model owner assigning identity information to the model user, which is then encoded into identity information codes with redundancy using Turbo codes. These identity information codes undergo encoding by the encoder, denoising of latent variables, inversion of latent variables, extraction of watermark information and error correction of the extracted identity information redundancy codes to restore the initial identity information. The mechanism of error correction codes combines partial watermark regions into a unified part, correcting the initial latent variables located at the boundaries of watermark detection regions, thereby enhancing the robustness of watermark detection.

5 THEORETICAL ANALYSIS OF THE PROPOSED SCHEME

5.1 Unified Representations of Watermark Regions and Latent Variables

Based on the initial requirements, we aim to establish a unified representation for watermark information and latent variable regions. For each watermark W , specific distributions of latent variables are distributed. These settings ensure that all images generated by the model can be attributed to the initial distribution of latent variables. Formally, We set both the diffusion model and the watermark model to share the same latent space. For specific parts of this latent space, we can sample and extract watermark features based on a probability function $P(z)$. We assume a series of deterministic functions $f(z; \theta)$ parameterized by a vector θ in some space Φ , where $f : Z \times \Phi \rightarrow X$. When θ is fixed and $z \sim \mathcal{N}(1, 0)$, $f(z; \theta)$ can generate latent variables that conform to a standard Gaussian distribution. By adopting this approach, we can construct watermark distribution regions corresponding to specific watermark information. These regions coincide with the latent variables of the diffusion model, achieving a unified representation of both. Additionally, the distribution of the watermark conforms to a standard normal distribution. This embedding process solely alters the selection of initial latent variables, preserving semantic consistency and image quality.

We aim to optimize θ such that $P(z)$ can be sampled z from while ensuring it closely matches the watermark W . To formalize this concept mathematically, the objective of DiffuseTrace is to maximize the probability of each W throughout the entire watermark extraction process. This objective stems from the principle of maximum likelihood. If the decoder is capable of reconstructing the watermark from the latent variables, it is also likely to reconstruct watermark from similar samples and unlikely to reconstruct watermark from dissimilar ones. To illustrate the dependence of $P(z)$ on W , we transform $f(z, \theta)$ into $P(W|z; \theta)$. The probability density function can be formalized as follows:

$$P(W) = \sum_z P(W|z; \theta)P(z) \quad (13)$$

The output distribution conforms to a Gaussian distribution after watermark embedding. Therefore, $P(W|z; \theta)$ satisfies the following distribution:

$$P(W|z; \theta) = \mathcal{N}(W|f(z; \theta), \sigma^2 I) \quad (14)$$

After embedding the watermark, the latent variables have a mean of $f(z; \theta)$ and a covariance equal to the identity matrix I multiplied by the scalar σ which is a hyperparameter.

5.2 The Implicit Allocation of Watermarks

Essentially, we need to partition the standard normal distribution, with each partition capable of accurately reconstructing the original watermark. For a 48-bit watermark, dividing into over two hundred eighty-one trillion regions presents a challenge in manually determining the watermark encoding regions given the complexity of explicitly partitioning watermark regions under the standard normal distribution. This implicit partitioning problem is analogous to the challenges faced by variational autoencoders in fitting distributions to data. As outlined in the paper [11], any distribution in d dimensions can be generated using a set of d variables drawn from a normal distribution and mapped through a sufficiently complex function. For $P(W)$, within the partitioning of the watermark into over two hundred eighty-one trillion blocks, most sampled z contribute minimally to $P(W)$, since $P(W|z)$ is close to zero for most z .

The approximation of the prior distribution can be simplified by introducing the posterior distribution $q(z|x)$. By computing the KL divergence between the posterior and prior distributions, we obtain:

$$D[q(z|w)||p(z|w)] = \mathbb{E}_{z \sim q}[z|w] - \log p(z|w) \quad (15)$$

The same of solving the variational evidence lower bound, we derive the watermark reconstruction evidence lower bound through Bayesian transformation:

$$\log p(w) \geq \mathbb{E}_{z \sim q}[\log p(w|z)] - D[q(z|w)||p(z)] \quad (16)$$

The first term in the equation represents maximizing the expected probability distribution of the watermark w given the latent variable z , i.e., the loss incurred by the watermark decoder in reconstructing the watermark. The second term is for the approximate posterior distribution of the latent space z to closely resemble the prior distribution, i.e., the watermark information generated by the encoder and the standard normal distribution should be as similar as possible.

5.3 Offset of Watermark Detection Region

As stated in Equation 7, diffusion inversion attributes the generated image to the initial latent variables. The assumption of diffusion inversion approximates $X_{t-1} - X_t$ to $X_{t+1} - X_t$. While unconditional diffusion inversion can yield accurate results, excessive guidance scale in conditional diffusion amplifies the errors introduced by null-text diffusion inversion [23]. In fact, after extracting the semantic embeddings of the images, conducting a forward pass after each inversion and applying gradient descent can enhance the effectiveness of the inversion process. Let the current latent variable be Z_{t_i} . $Z_{t_{i+1}}$ is obtained after performing inversion on Z_{t_i} . The process of solving $Z_{t_{i+1}}$ under the guidance of extracting semantic embeddings can be mathematically expressed as follows:

$$\nabla_{z_{t_{i+1}}} \|z_{t_i} - z'_{t_i}\|_2^2 \quad (17)$$

Theoretically, refining the decoder by restoring the initial latent variables through the aforementioned approach would yield better results. However, considering the computational overhead of the gradient descent process, the approach adopted in the paper accepts the inaccuracy of diffusion inversion under zero text and defines this inaccuracy as the offset to the watermark detection region. The purpose of fine-tuning is to learn the offset vector as p . The watermark encoder trained with maximum likelihood exhibits the following properties, similar samples have more similar latent variables, while dissimilar samples have greater distances in the latent space. The distance between the similar latent variables obtained after inversion and the initial latent variables should be less than a certain threshold ϵ to guarantee the accuracy of detection. After the watermark region is segmented, the watermark detection area is offset due to diffusion inversion, the refinement target at this point transforms into:

$$\min_{\theta} \mathbb{E}_{(x_i, y_i) \sim \mathcal{D}} [\max L(\theta, \text{inv}(\text{deno}(x_i)) + p_i, y_i)]. \quad (18)$$

x_i denotes specific latent variables and y_i denotes the watermark region x_i belong. In the formula 19, deno represents the process of diffusion denoising 6, inv represents the precise inversion process, and p_i denotes the offset of the watermark detection area caused by approximation 7. After fine-tuning the watermark decoder, it should satisfy $p < \epsilon$ to ensure detection accuracy. Taking into account that images may undergo various treatments including image blurring, Gaussian noise, color transformations, etc., such attacks can affect samples on the edges of the watermark region, leading to decreased detection accuracy. Essentially, this process does not alter the watermark's region, but it notably aids in repairing the evasion of edge samples. Adversarial training can appropriately expand the range of the watermark detection region for various attacks. Therefore, the refinement target can be further transformed into:

$$\min_{\theta} \mathbb{E}_{(x_i, y_i) \sim \mathcal{D}} [\max L(\theta, \text{inv}(\text{deno}(x_i)) + \delta) + p_i, y_i)]. \quad (19)$$

The variable δ can be expressed as the deviations caused by various attacks on the image, where images generated after such attacks are semantically similar but deviate from the original image in semantic space. Correcting this step further enhances the watermark decoder's detection accuracy for edge samples.

5.4 Security Analysis

Based on the above analysis, DiffuseTrace divides the watermark region into multiple contiguous areas. Assuming the image undergoes image processing resulting in changes compared to the original image, this change is assumed to be ϵ_p within the latent variable space. The initial latent variable corresponding to the original image is $Z_0 \in X$. As long as $Z_T + \epsilon_p \in X$, the watermark verification is successful. For the initial latent variables close to the center of the watermark region, the distance from the latent variables to other watermark regions is $D \gg \epsilon_p$. In this case, watermark verification is straightforward. However, for samples at the edges of the watermark region, $Z_T + \epsilon_p \notin X$. In the detection phase, we effectively expanded the detection area for each watermark, considering the outer radius r of each watermark region as part of the region itself. This process can be formalized as follows:

$$\text{detect}(z_T + \epsilon_p) = \text{judge}(z_0 + \epsilon_p \in (X + r)) \quad (20)$$

The size of r depends on the magnitude of the perturbations in adversarial samples used during adversarial training. Expanding the partition of watermark regions actually increases the risk of overlap to some extent between different watermark regions.

We set the distance d between the two watermark regions. Since the encoder remains fixed, the region of the watermark itself won't change. However, due to inversion-induced overall shifts and image processing, the detection area post-inversion corresponds to a deviated initial region. If $r \leq d$, adversarial training enhances the robustness of the watermark, ensuring that even edge latent variables can still extract the watermark.

Security Analysis Without Attack. If the magnitude of adversarial training r exceeds d , it causes the watermark from one edge sample to fall within the detection range of another, leading to bit errors. Indeed, during training, adversarial samples at the boundary regions steer the model in the wrong direction, while correct samples in these regions guide the model back on track. As a result, the accuracy of samples in these areas remains above fifty percent but unstable, leading to a fluctuating state. To correct such errors, we employ error correction codes. As mentioned by 4.4, if the error rate of samples in the boundary region is within an acceptable range, error correction codes can restore the original information. Essentially, this approach uses a larger amount of information to rectify errors and merges multiple regions into one.

Security Analysis of Image Processing. In our scheme, we consider image manipulation where the same image undergoes a certain offset in the latent space, but within an acceptable range smaller than a certain threshold. If the corresponding change in the latent space is less than d , adversarial training ensures that both central and marginal latent variables can successfully decode the information. Common image manipulations such as Gaussian transformations, color jittering, brightness variations and image compression all keep the image's position in the latent space within an acceptable range. Therefore, DiffuseTrace effectively defends against such attacks. Even with significant image manipulations such as JPEG compression to 10 percent, contrast increase to 8, and brightness increase to 6, DiffuseTrace maintains a certain level of accuracy.

Security Analysis of VAE-based Attacks and Diffusion-based Attacks. The core idea behind attacks such as VAE-based

attacks and Diffusion-based attacks in the proposed scheme is to disrupt and reconstruct. Disruption involves adding noise to the image, while reconstruction involves removing the noise through a diffusion model.

The reason why such attacks can succeed is that the primary objective of most watermarking schemes is to add minimal watermark noise to the image while still being able to extract the watermark information. These methods often utilize the LPIPS loss [47] or differences in the color channels of the image as the loss function, aiming to minimize the SSIM and PSNR metrics of the final image. This allows reconstruction attacks to exploit this vulnerability by continuously adding noise to gradually degrade the stability of the watermark. Eventually, the reconstruction process generates an image that is indistinguishable from the watermark. While some watermarking schemes, such as Stegastamp, sacrifice image quality and significantly increase adversarial training to enhance their stability, there is no defense against reconstruction attacks when constructive steps become sufficiently numerous. In fact, reconstruction attacks can even produce images that are clearer than the watermark samples.

The watermark based on the initial latent variables primarily operates at the semantic level, allowing for stable watermark extraction as long as there are no significant changes in the image within the latent space. Attacks on watermarks based on diffusion models by adding noise do not alter the original semantic content of the image actually. The initial hidden space positions of the image can still be discerned which makes it resistant to such reconstruction attacks. This is exactly the advantage of DiffuseTrace in combating attacks.

6 EXPERIMENTS

6.1 Experimental settings

Datasets. In the experiment, we utilized the following datasets:

- **Real Photos:** 500 images were randomly selected from MSCOCO [18], which contains over 328K images along with their annotations.
- **AI-Generated Images Prompts:** 500 prompts were randomly sampled from Diffusion Prompts, a database of approximately 80,000 prompts filtered and extracted from image finders.
- **AI-Generated Images:** 500 images and prompts are randomly chosen from StableDiffusionDB [41]. This dataset contains images generated by Stable Diffusion based on prompts and hyperparameters provided by actual user interactions.

Watermark Baselines. For traditional watermarking schemes, we selected DcTDwt [1] and DcTDwtSvD [8] which is deployed in Stable Diffusion as a watermark with an embedding capacity of 48. For post-processing watermarking schemes based on Encoder-Decoder/GAN structures, we chose RivaGAN [44], Hidden [51] and StegaStamp [37] with embedding capacities of 32, 48, 48, and 48 respectively. For watermarking schemes based on Variational Autoencoders, we chose Stable Signature [13] and SSLWatermark [14] with an embedding capacity of 48. Additionally, for watermarking schemes based on latent variables, we chose Tree-Ring with a watermark radius of 10. Given that tree-ring is a zero-bit watermark scheme, we utilized p-values as the detection metric. The

Table 1: Bit Accuracy/Detection Accuracy Under Image Processing

Method	Brightness	Noise	Contrast	Hue	JPEG	Blur	Resize	BM3D	
Value	2.0	0.05	2.0	0.25	50	7*7	0.3	30	
Traditional Wm.	DwtDct	0.601/0.000	0.801/0.642	0.497/0.000	0.479/0.000	0.488/0.000	0.582/0.092	0.493/0.000	0.498/0.000
	D.Svd	0.612/0.042	0.850/ 0.999	0.718/0.118	0.485/0.000	0.498/0.000	0.989/ 0.999	0.506/0.000	0.632/0.084
Enc.-Dec. Wm.	RivaGan	0.975/ 0.999	0.960/0.994	0.832/0.992	0.984/ 0.999	0.773/0.801	0.867/0.924	0.504/0.000	0.858/0.873
	Hidden	0.964/ 0.999	0.971/0.994	0.979/ 0.999	0.992/ 0.999	0.849/0.823	0.816/0.852	0.825/0.873	0.626/0.168
	S.Stamp	0.937/ 0.999	0.979/ 0.999	0.972/ 0.999	0.995/ 0.999	0.952/ 0.999	0.981/ 0.999	0.972/ 0.999	0.980/ 0.999
VAE-Based Wm.	S.Signa	0.971/ 0.999	0.976/0.996	0.965/ 0.999	0.954/0.994	0.806/0.809	0.781/0.822	0.513/0.011	0.604/0.013
Latent-Based Wm.	SSLWm.	0.927/ 0.999	0.627/0.124	0.975/ 0.999	0.942/0.997	0.547/0.000	0.997/ 0.999	0.844/0.901	0.620/0.224
	Ours	0.942/ 0.999	0.915/ 0.999	0.959/ 0.999	0.982/ 0.999	0.912/ 0.999	0.966/ 0.999	0.922/ 0.999	0.902/ 0.999

Table 2: Image Sematic Quality and Undetectability Evaluation. The table demonstrates the impact of adding semantic watermarks on image quality through two No-inference Metrics, NIQE and PIQE. The semantic consistency before and after adding the DiffuseWatermark is evaluated through the Clip metric.

Dataset	Method	NIQE↓	PIQE↓	Clip↑	Bit/Detect
DiffusionDB	No-Watermark	4.91	28.21	0.342	0.511/0.000
	Tree-ring(rad10)	5.32	30.28	0.332	-/0.999
	Tree-ring(rad20)	6.64	37.33	0.301	-/0.999
	DiffuseTrace(16)	4.22	29.08	0.344	0.999/0.999
	DiffuseTrace(32)	5.04	29.77	0.339	0.992/0.999
	DiffuseTrace(48)	4.72	28.41	0.340	0.984/0.999
MS-COCO Prompts	No-Watermark	3.85	33.28	0.335	0.504/0.000
	Tree-ring(rad10)	4.32	34.28	0.324	-/0.999
	Tree-ring(rad20)	5.64	38.33	0.291	-/0.999
	DiffuseTrace(16)	4.12	33.25	0.333	0.999/0.999
	DiffuseTrace(32)	3.81	30.21	0.326	0.994/0.999
	DiffuseTrace(48)	4.17	32.34	0.330	0.990/0.999
Diffusion Prompts	No-Watermark	4.88	29.72	0.326	0.488/0.999
	Tree-ring(rad10)	5.32	30.28	0.327	-/0.999
	Tree-ring(rad20)	5.94	37.33	0.303	-/0.999
	DiffuseTrace(16)	4.93	28.42	0.358	0.999/0.999
	DiffuseTrace(32)	5.11	30.18	0.353	0.999/0.999
	DiffuseTrace(48)	4.70	26.33	0.328	0.984/0.999

corresponding bit capacity of DiffuseTrace is 48 bits. Considering the additional overhead of redundancy codes, no error correction codes were used in the comparative experiments.

Attack Baselines. To thoroughly evaluate the robustness of DiffuseTrace, we test it against a comprehensive set of baseline attacks that represent common image processing, VAE-based attack and diffusion-based attack. Specially, The set of attacks employed in our testing includes:

- brightness and contrast change of 2.0
- addition of Gaussian noise with standard deviation of 0.05
- Adjustment of the hue by 0.25.
- JPEG compression with a quality setting of 50.
- BM3D denoising algorithm with Peak Signal-to-Noise Ratio Standard Deviation of 30.

- Gaussian blur with kernel size 7 and standard deviation of 1
- Two Variational AutoEncoder (VAE) based image compression models, Bmshj18 [2] and Cheng20 [7], both with compression factors of 3.
- A stable diffusion-based image regeneration model for watermark attack, Zhao23 [49] with 40 denoising steps.

Evaluation Metrics. The two main objectives of incorporating watermarks are copyright protection and user tracing. Therefore, we utilize *pvalue* as the standard for copyright tracing and utilize bit accuracy rate as the standard for user tracing. We set a decision threshold to reject the null hypothesis for $p < 0.01$, requiring detection of the corresponding method-corrected 24/32 and 34/48 bits. Otherwise, the image is deemed to be without a watermark.

Semantic consistency. Since our images have watermarks added before image generation, the watermark is reflected at the semantic level. Therefore, we choose the CLIP score metric [25] to evaluate the semantic consistency between generated images and prompt words. The reference metric will be used to evaluate the semantic quality difference between the generated images with and without watermark embedding in DiffuseTrace in order to evaluate the fidelity of watermark embedding

Image Quality. We evaluate the quality of an image through two no-reference metrics, the Natural Image Quality Evaluator (NIQE) score [22] and the Perceptual Image Quality Evaluator (PIQE) score [38]. The reference indicators will be used to compare the quality of images without watermarks with images with watermarks embedded in order to evaluate the loss of watermark embedding on the image and the invisibility of the watermark.

6.2 Sematic and image quality evaluation

From Table 2, we evaluated the impact of embedding the watermark on image quality and semantic consistency before and after. The experiment utilized the stable-diffusion-2-1-base model [29] with 25 inference steps at the guidance scale of 5. Results indicate no significant differences in NIQE and PIQE quality metrics across different watermark bits. Additionally, semantic alignment of generated images, as assessed by Clip scores, remains similar to the original model. This suggests that DiffuseTrace does not rely on the trade-off between image quality and watermark robustness typical of post-processing watermarks. Since images are generated

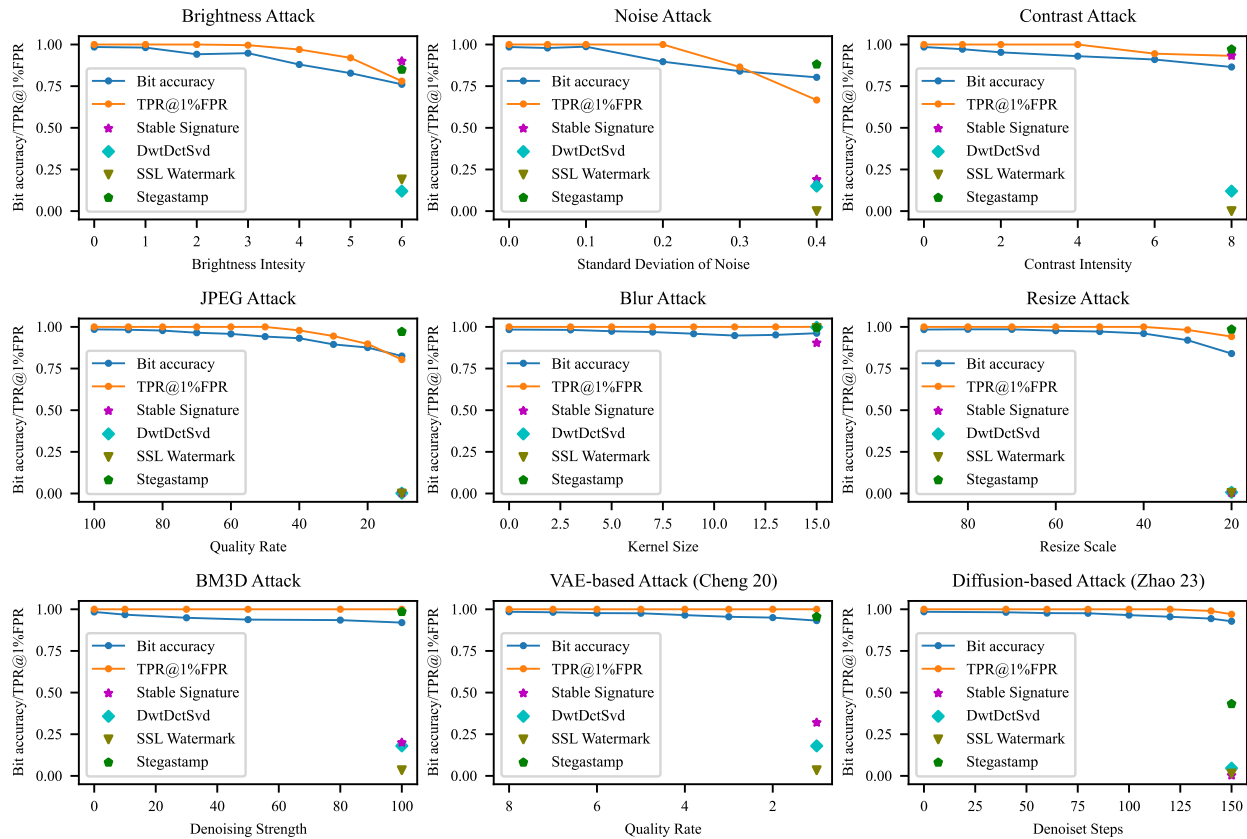


Figure 2: The figure illustrates the performance of DiffuseTrace in response to various attacks of different intensities, measured by bit accuracy and TPR@0.01FPR. It also compares TPR@0.01FPR of traditional watermarks such as DwtDetSvd, SSL Watermark and Stable Signaturez under corresponding attacks. The watermark capacity for each scheme in the figure is 48 bits.

entirely through correct sampling processes and variables are properly distributed without subsequent modifications to the images, the DiffuseTrace approach exhibits significant advantages in terms of image quality compared to post-processing solutions. Compared to other methods that embed watermarks in the latent space, the SSL watermark remains a post-processing solution. Tree-ring alters the distribution of initial latent variables by embedding the watermark in the frequency domain of the latent space through Fourier transformation. However, U-net fails to recover from the losses incurred during this process. Consequently, as the watermark radius increases, the generated images suffer significant losses in both quality and semantic consistency.

6.3 Robustness evaluation against image processing

From Table 1, we evaluated the robustness of the watermark against various image processing attacks. It could be observed from the graph that DiffuseTrace demonstrates stability and robustness when faced with common image processing attacks. DiffuseTrace achieve watermark detection rate close to 100 percent and average bit accuracy above 90 percent under common attack. Compared to

post-processing watermarking schemes and VAE-based watermarking schemes, DiffuseTrace demonstrates excellent stability when faced with significant image compression and resizing. Stegastamp remain highly robust in the comparison, since it sacrifices image quality and utilizes error correction codes to compress 96 bits into 48 bits, with a relatively large error correction space. Stable Signature watermark specially for diffusion model remain stable under most attacks, but is vulnerable to denoise algorithm and processing to high extent. Furthermore, We conducted detailed experiments on various types of image disturbance amplitudes and compared the current method to latent-based method ssl watermark and vae-based watermark stable signature under maximum attack intensity. The results showed that DiffuseTrace has a significant advantage in image processing stability compared to other methods.

6.4 Robustness evaluation against VAE-based attacks and diffusion based attacks.

In Table 3, we evaluated the accuracy of various watermarking schemes when faced with deep learning-based attacks. The experiments consist of VAE-based attack and diffusion-based attack which is the latest watermark attack. The table reveals that the majority of

schemes are unable to withstand this type of reconstruction attack. Stable Signature exhibits fragile. From the results, it is evident that DiffuseTrace exhibits a significant advantage in countering VAE-based attacks utilizing diffusion models. SSL watermarks and stable signatures all exhibit low watermark detection rates, indicating that they are unable to resist both VAE-based and diffusion based attacks. For diffusion based attacks, except for DiffuseTrace, other watermark schemes have experienced a significant drop in bit accuracy. In subsequent experiments, we increased the intensity of the diffusion attack. From the results, it is evident that DiffuseTrace exhibits significantly higher resilience against reconstruction attacks compared to other methods. Even the VAE-attack with a quality coefficient of 1 or the diffusion-based attack with 150 denoise steps do not fundamentally affect the stability of the watermark and only the DiffuseTrace was able to maintain accuracy in high-intensity reconstruction. Reconstruction attacks are achieved by maintaining semantic accuracy, continuously adding noise to destroy watermarks and continuously reconstructing and restoring images to obtain images without watermarks. However, this process essentially does not alter the semantic consistency of the image nor does it significantly alter the initial latent variables of image inversion. Therefore, DiffuseTrace can remain stable under reconstruction attacks.

Table 3: Bit Accuracy/Detection Accuracy Under Deep-learning-based Attack

Method		VAE A.		Diffusion A.
		Bmshj18 [2]	Cheng20 [7]	Zhao23 [49]
Traditional Wm.	DwtDct	0.524/0.000	0.517/0.012	0.489/0.000
	D.Svd	0.504/0.000	0.512/0.013	0.523/0.014
Enc.-Dec. Wm.	RivaGan	0.611/0.063	0.632/0.070	0.588/0.070
	Hidden	0.621/0.170	0.641/0.198	0.497/0.009
	S.Stamp	0.979/1.000	0.965/1.000	0.852/0.927
VAE-based Wm.	Stable Signature	0.616/0.224	0.682/0.409	0.541/0.014
Latent-based Wm.	SSL Wm.	0.623/0.123	0.631/0.144	0.655/0.149
	Tree-ring	- /0.993	- /0.991	- /0.997
	Ours	0.972/1.000	0.967/1.000	0.970/1.000

6.5 Ablation Experiments

This section, we experimentally quantify the impact of several key hyperparameters mentioned in the theoretical analysis 5 on the inaccuracy. we consider the impact of the guidance scale used during the generation phase, the inference steps employed during the inversion phase, and the version of the model on watermark detection in order to demonstrate the effectiveness of DiffuseTrace.

Ablation on Guidance Scale. In the theoretical analysis 5.3, we elaborate on the reasons why the guidance scale introduces errors into the experiments. In the following experiments, we quantify the impact of the guidance scale on the DiffuseTrace watermarking scheme through experimentation. For the ablation experiment on the guidance scale, the scheduler is set the dpm++ [20] scheduler. The experimental setup includes setting both the inference steps and reverse inference steps to 20. We adjust the guidance scale to assess its influence on the experimental results.

The specific experimental results depicted in the graph 3 show that as the guidance scale increases during the inference stage, the bit accuracy gradually decreases, while the detection accuracy remains relatively stable within the guidance scale range of 0 to 20. This indicates that the watermark detection accuracy is maintained, demonstrating the robustness of the watermark. Thus, users can freely adjust the guidance scale during the image generation stage while still ensuring traceability of the watermark. Deploying the diffusion model as a service can provide users with the option to adjust the guidance scale hyperparameter, which will not significantly affect watermark detection.

Ablation on Inference Steps. The ablation experiment for reverse inference steps employed the DPM++ scheduler, with an inference step setting of 20 and a guidance scale set to 5. The evaluation of the experiment’s results involves adjusting the reverse inference steps to assess their impact.

The experimental results, as depicted in the figure 3, indicate that after 5 inference steps of inversion, the watermark detection rate stabilizes. Even with only 2 inference steps, a good detection rate can still be maintained. This suggests that the number of inference steps does not significantly affect the accuracy of detection. Therefore, during the detection phase, to increase efficiency, a small number of reverse inference steps can be employed to extract the image watermark.

7 RELATED WORK

7.1 Detection of AI-Generated Images

It is difficult for humans to distinguish between real and fake images. Realistic fake images intensify concerns about the disinformation dissemination. To tackle this problem, various fake image detection approaches have been proposed. A typical approach [15, 36, 39] involves extracting temporal, frequency, and texture features from images. Subsequently, a feature extraction network is constructed to train a binary classifier to distinguish between AI-generated images and real images. However, this image detection method exhibits noticeable performance degradation when applied to diffusion models. For AI-generated image detection based on diffusion models [40], leveraging a pre-trained diffusion model allows for a more accurate reconstruction of the characteristics of images generated through the diffusion process. By reconstructing the diffusion process, differences between real images and images generated by the diffusion model can be detected thereby enabling the detection of AI-generated images. Adding a watermark to generated images is also a method for identifying AI-generated images.

7.2 Image Watermarking

The strategy of adding watermarks to images for protecting intellectual property rights has a long history in the field of computer vision. Traditional image watermarking methods typically involve embedding watermarks into appropriate frequency components of the image, utilizing techniques such as Discrete Cosine Transform (DCT), Discrete Wavelet Transform (DWT) [1] or Singular Value Decomposition (SVD) [19]. Deep learning-based approaches, such as HiDDeN [51], StegaStamp [37], have demonstrated competitive results in terms of robustness against various geometric

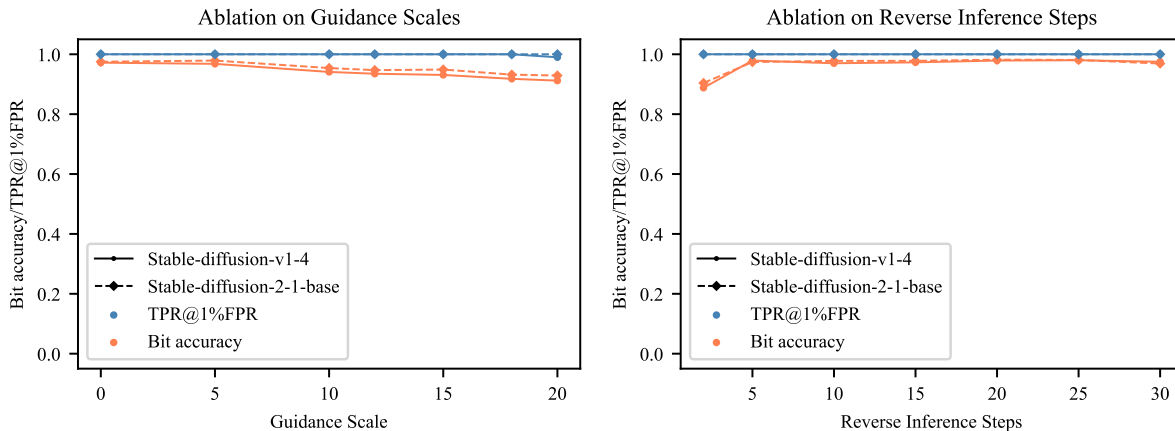


Figure 3: The figure (left) illustrates the ablation experiment concerning the guidance scale, where adjusting the guidance scale leads to a gradual decrease in the watermark’s bit accuracy, while the watermark detection rate remains stable. The figure (right) shows the results of the ablation study on reverse inference steps, where the bit rate detected stabilizes after two inference steps.

transformations. These methods often employ deep learning encoders and extractors to embed and extract watermarks respectively. The aforementioned watermarking methods primarily focus on post-processing existing images. The core idea is to achieve robustness against various attacks while minimizing the impact on the visual quality of the image. Therefore, post-processing methods are confronted with a trade-off between watermark stability, watermark capacity and image quality.

For diffusion model watermarking, it can mainly be categorized into three types:

Watermark embedding during training phase. In methods incorporating watermarks during the training phase, watermarks are embedded into the training data. The data is encoded with the watermark during training and a decoder is trained to extract the watermark. During the detection phase, all images generated by diffusion models will carry encoded binary strings. Watermark [50] is a representative approach. Methods of this kind typically have stringent requirements for watermark embedding, involving the incorporation of watermarks into a substantial dataset of images followed by training the entire model.

Fine-tuning phase with watermark incorporation. The main purpose of such watermark embedding methods is to integrate the watermark component into the model component, making it inseparable during distribution. Watermarks are incorporated into model components during fine-tuning. For instance, methods like Stable Signature [13] and FSwatermark [43] fine-tune the variational autoencoders to ensure that all generated images carry the watermark. It’s approximate to integrating the watermark into the final generation stage.

Watermark embedding into latent space during inference. During inference steps, watermarks are added to the latent variable space of the model. Methods like Tree-ring [42] and ZoDiac [45] achieve this by diffusing inversion and applying frequency domain

transformations to latent variables, ensuring that all generated images carry the watermark. DiffuseTrace also falls into this category of methods. The watermark is embedded in the image prior to its generation.

7.3 Image Watermarking Attack

The goal of image watermark attacks is to assess the robustness of image detection after practical modifications. These attacks mainly fall into two categories: image processing attacks and deep learning-based attacks.

image processing attacks. Common image processing techniques include adding noise, color jitter, image compression, image scaling and Gaussian blur. Image processing or compression methods may utilize frequency-domain or 3D transformation-based approaches including BM3D denoising algorithm [9].

Deep learning-based attack. Deep learning-based attack methods, including methods based on variational autoencoders such as [2] and [7] can disrupt watermarks embedded in images. In recent research, diffusion based attacks [49] are used to encode the semantic features of images, add noise to disrupt watermark and regenerate images. Reconstruction models exhibit prominent performance and can eliminate most watermarks injected by most existing methods.

8 CONCLUSION

In this paper we propose DiffuseTrace, a plug-in multibit watermarking module to protect copyright of diffusion models and trace generated images semantically. DiffuseTrace extends semantic image watermarking of latent diffusion models further into multi-bit scenarios. DiffuseTrace does not rely on the balance between image quality and watermark robustness and has significant advantages in

image quality compared to previous watermarking schemes. Compared to state-of-the-art schemes, DiffuseTrace demonstrates prominent performance against variational autoencoders and diffusion-based watermark attacks. Due to its flexibility and generalizability, DiffuseTrace can be seamlessly applied to copyright protection in diffusion models, recognition of machine-generated images, and user traceability in machine-generated image services. We assess the security of the watermarking scheme through theoretical analysis and demonstrate its robustness against image processing attacks and state-of-the-art image watermarking attack schemes through experiments.

REFERENCES

- [1] Ali Al-Haj. 2007. Combined DWT-DCT digital image watermarking. *Journal of Computer Science* 3, 9 (2007), 740–746.
- [2] Johannes Ballé, David Minnen, Saurabh Singh, Sung Jin Hwang, and Nick Johnston. 2018. Variational image compression with a scale hyperprior. *arXiv preprint arXiv:1802.01436* (2018).
- [3] Claude Berrou, Alain Glavieux, and Punya Thitimajshima. 1993. Near Shannon limit error-correcting coding and decoding: Turbo-codes. 1. In *Proceedings of IEEE International Conference on Communications*, Vol. 2. IEEE, 1064–1070.
- [4] Andreas Blattmann, Robin Rombach, Huan Ling, Tim Dockhorn, Seung Wook Kim, Sanja Fidler, and Karsten Kreis. 2023. Align your latents: High-resolution video synthesis with latent diffusion models. In *Proceedings of the IEEE/CVF Conference on Computer Vision and Pattern Recognition*. 22563–22575.
- [5] Tim Brooks, Aleksander Holynski, and Alexei A Efros. 2023. Instructpix2pix: Learning to follow image editing instructions. In *Proceedings of the IEEE/CVF Conference on Computer Vision and Pattern Recognition*. 18392–18402.
- [6] Taylan Cemgil, Sumedh Ghaisas, Krishnamurthy Dvijotham, Sven Gowal, and Pushmeet Kohli. 2020. The autoencoding variational autoencoder. *Advances in Neural Information Processing Systems* 33 (2020), 15077–15087.
- [7] Zhengxue Cheng, Heming Sun, Masaru Takeuchi, and Jiro Katto. 2020. Learned image compression with discretized gaussian mixture likelihoods and attention modules. In *Proceedings of the IEEE/CVF Conference on Computer Vision and Pattern Recognition*. 7939–7948.
- [8] Ingemar Cox, Matthew Miller, Jeffrey Bloom, Jessica Fridrich, and Ton Kalker. 2007. *Digital watermarking and steganography*. Morgan Kaufmann.
- [9] Kostadin Dabov, Alessandro Foi, Vladimir Katkovnik, and Karen Egiazarian. 2007. Image denoising by sparse 3-D transform-domain collaborative filtering. *IEEE Transactions on Image Processing* 16, 8 (2007), 2080–2095.
- [10] Prafulla Dhariwal and Alexander Nichol. 2021. Diffusion models beat gans on image synthesis. *Advances in Neural Information Processing Systems* 34 (2021), 8780–8794.
- [11] Carl Doersch. 2016. Tutorial on variational autoencoders. *arXiv preprint arXiv:1606.05908* (2016).
- [12] Patrick Esser, Robin Rombach, and Bjorn Ommer. 2021. Taming transformers for high-resolution image synthesis. In *Proceedings of the IEEE/CVF Conference on Computer Vision and Pattern Recognition*. 12873–12883.
- [13] Pierre Fernandez, Guillaume Couairon, Hervé Jégou, Matthijs Douze, and Teddy Furon. 2023. The stable signature: Rooting watermarks in latent diffusion models. In *Proceedings of the IEEE/CVF International Conference on Computer Vision*. 22466–22477.
- [14] Pierre Fernandez, Alexandre Sablayrolles, Teddy Furon, Hervé Jégou, and Matthijs Douze. 2022. Watermarking images in self-supervised latent spaces. In *ICASSP 2022–2022 IEEE International Conference on Acoustics, Speech and Signal Processing*. IEEE, 3054–3058.
- [15] Joel Frank, Thorsten Eisenhofer, Lea Schönherr, Asja Fischer, Dorothea Kolossa, and Thorsten Holz. 2020. Leveraging frequency analysis for deep fake image recognition. In *International conference on Machine Learning*. PMLR, 3247–3258.
- [16] Jonathan Ho, William Chan, Chitwan Saharia, Jay Whang, Ruiqi Gao, Alexey Gritsenko, Diederik P Kingma, Ben Poole, Mohammad Norouzi, David J Fleet, et al. 2022. Imagen video: High definition video generation with diffusion models. *arXiv preprint arXiv:2210.02303* (2022).
- [17] Jonathan Ho, Ajay Jain, and Pieter Abbeel. 2020. Denoising diffusion probabilistic models. *Advances in Neural Information Processing Systems* 33 (2020), 6840–6851.
- [18] Tsung-Yi Lin, Michael Maire, Serge Belongie, James Hays, Pietro Perona, Deva Ramanan, Piotr Dollár, and C Lawrence Zitnick. 2014. Microsoft coco: Common objects in context. In *Computer Vision—ECCV 2014: 13th European Conference, Zurich, Switzerland, September 6–12, 2014, Proceedings, Part V 13*. Springer, 740–755.
- [19] Junxian Liu, Jiadong Huang, Yuling Luo, Lvchen Cao, Su Yang, Duqu Wei, and Ronglong Zhou. 2019. An optimized image watermarking method based on HD and SVD in DWT domain. *IEEE Access* 7 (2019), 80849–80860.
- [20] Cheng Lu, Yuhao Zhou, Fan Bao, Jianfei Chen, Chongxuan Li, and Jun Zhu. 2022. Dpm-solver++: Fast solver for guided sampling of diffusion probabilistic models. *arXiv preprint arXiv:2211.01095* (2022).
- [21] Andreas Lugmayr, Martin Danelljan, Andres Romero, Fisher Yu, Radu Timofte, and Luc Van Gool. 2022. Repaint: Inpainting using denoising diffusion probabilistic models. In *Proceedings of the IEEE/CVF Conference on Computer Vision and Pattern Recognition*. 11461–11471.
- [22] Anish Mittal, Rajiv Soundararajan, and Alan C Bovik. 2012. Making a “completely blind” image quality analyzer. *IEEE Signal Processing Letters* 20, 3 (2012), 209–212.
- [23] Ron Mokady, Amir Hertz, Kfir Aberman, Yael Pritch, and Daniel Cohen-Or. 2023. Null-text inversion for editing real images using guided diffusion models. In *Proceedings of the IEEE/CVF Conference on Computer Vision and Pattern Recognition*. 6038–6047.
- [24] Alex Nichol, Prafulla Dhariwal, Aditya Ramesh, Pranav Shyam, Pamela Mishkin, Bob McGrew, Ilya Sutskever, and Mark Chen. 2021. Glide: Towards photorealistic image generation and editing with text-guided diffusion models. *arXiv preprint arXiv:2112.10741* (2021).
- [25] Alec Radford, Jong Wook Kim, Chris Hallacy, A. Ramesh, Gabriel Goh, Sandhini Agarwal, Girish Sastry, Amanda Askell, Pamela Mishkin, Jack Clark, Gretchen Krueger, and Ilya Sutskever. 2021. Learning Transferable Visual Models From Natural Language Supervision. In *ICML*.
- [26] Aditya Ramesh, Prafulla Dhariwal, Alex Nichol, Casey Chu, and Mark Chen. 2022. Hierarchical text-conditional image generation with clip latents. *arXiv preprint arXiv:2204.06125* 1, 2 (2022), 3.
- [27] Aditya Ramesh, Mikhail Pavlov, Gabriel Goh, Scott Gray, Chelsea Voss, Alec Radford, Mark Chen, and Ilya Sutskever. 2021. Zero-shot text-to-image generation. In *International Conference on Machine Learning*. Pmlr, 8821–8831.
- [28] Robin Rombach, Andreas Blattmann, Dominik Lorenz, Patrick Esser, and Björn Ommer. 2022. High-resolution image synthesis with latent diffusion models. In *Proceedings of the IEEE/CVF Conference on Computer Vision and Pattern Recognition*. 10684–10695.
- [29] Robin Rombach, Andreas Blattmann, Dominik Lorenz, Patrick Esser, and Björn Ommer. 2022. High-Resolution Image Synthesis With Latent Diffusion Models. In *Proceedings of the IEEE/CVF Conference on Computer Vision and Pattern Recognition (CVPR)*. 10684–10695.
- [30] Olaf Ronneberger, Philipp Fischer, and Thomas Brox. 2015. U-net: Convolutional networks for biomedical image segmentation. In *Medical Image Computing and Computer-assisted Intervention—MICCAI 2015: 18th international conference, Munich, Germany, October 5–9, 2015, proceedings, part III 18*. Springer, 234–241.
- [31] Chitwan Saharia, William Chan, Huiwen Chang, Chris Lee, Jonathan Ho, Tim Salimans, David Fleet, and Mohammad Norouzi. 2022. Palette: Image-to-image diffusion models. In *ACM SIGGRAPH 2022 Conference Proceedings*. 1–10.
- [32] Chitwan Saharia, William Chan, Saurabh Saxena, Lala Li, Jay Whang, Emily L Denton, Kamyar Ghasemipour, Raphael Gontijo Lopes, Burcu Karagol Ayan, Tim Salimans, et al. 2022. Photorealistic text-to-image diffusion models with deep language understanding. *Advances in Neural Information Processing Systems* 35 (2022), 36479–36494.
- [33] Chitwan Saharia, Jonathan Ho, William Chan, Tim Salimans, David J Fleet, and Mohammad Norouzi. 2022. Image super-resolution via iterative refinement. *IEEE Transactions on Pattern Analysis and Machine Intelligence* 45, 4 (2022), 4713–4726.
- [34] Jiaming Song, Chenlin Meng, and Stefano Ermon. 2020. Denoising diffusion implicit models. *arXiv preprint arXiv:2010.02502* (2020).
- [35] Yang Song, Jascha Sohl-Dickstein, Diederik P Kingma, Abhishek Kumar, Stefano Ermon, and Ben Poole. 2020. Score-based generative modeling through stochastic differential equations. *arXiv preprint arXiv:2011.13456* (2020).
- [36] Chuangchuang Tan, Yao Zhao, Shikui Wei, Guanghua Gu, and Yunchao Wei. 2023. Learning on gradients: Generalized artifacts representation for gan-generated images detection. In *Proceedings of the IEEE/CVF Conference on Computer Vision and Pattern Recognition*. 12105–12114.
- [37] Matthew Tancik, Ben Mildenhall, and Ren Ng. 2020. Stegastamp: Invisible hyperlinks in physical photographs. In *Proceedings of the IEEE/CVF Conference on Computer Vision and Pattern Recognition*. 2117–2126.
- [38] N Venkatanath, D Praneeth, Maruthi Chandrasekhar Bh, Sumohana S Channappayya, and Swarup S Medasani. 2015. Blind image quality evaluation using perception based features. In *2015 Twenty First National Conference on Communications*. IEEE, 1–6.
- [39] Sheng-Yu Wang, Oliver Wang, Richard Zhang, Andrew Owens, and Alexei A Efros. 2020. CNN-generated images are surprisingly easy to spot... for now. In *Proceedings of the IEEE/CVF Conference on Computer vision and pattern recognition*. 8695–8704.
- [40] Zhendong Wang, Jianmin Bao, Wengang Zhou, Weilun Wang, Hezhen Hu, Hong Chen, and Houqiang Li. 2023. Dire for diffusion-generated image detection. In *Proceedings of the IEEE/CVF International Conference on Computer Vision*. 22445–22455.
- [41] Zijie J Wang, Evan Montoya, David Munechika, Haoyang Yang, Benjamin Hoover, and Duen Horng Chau. 2022. Diffusiondb: A large-scale prompt gallery dataset for text-to-image generative models. *arXiv preprint arXiv:2210.14896* (2022).

- [42] Yuxin Wen, John Kirchenbauer, Jonas Geiping, and Tom Goldstein. 2023. Tree-ring watermarks: Fingerprints for diffusion images that are invisible and robust. *arXiv preprint arXiv:2305.20030* (2023).
- [43] Cheng Xiong, Chuan Qin, Guorui Feng, and Xinpeng Zhang. 2023. Flexible and secure watermarking for latent diffusion model. In *Proceedings of the 31st ACM International Conference on Multimedia*. 1668–1676.
- [44] Kevin Alex Zhang, Lei Xu, Alfredo Cuesta-Infante, and Kalyan Veeramachaneni. 2019. Robust invisible video watermarking with attention. *arXiv preprint arXiv:1909.01285* (2019).
- [45] Lijun Zhang, Xiao Liu, Antoni Viros Martin, Cindy Xiong Bearfield, Yuriy Brun, and Hui Guan. 2024. Robust Image Watermarking using Stable Diffusion. *arXiv preprint arXiv:2401.04247* (2024).
- [46] Lvmin Zhang, Anyi Rao, and Maneesh Agrawala. 2023. Adding conditional control to text-to-image diffusion models. In *Proceedings of the IEEE/CVF International Conference on Computer Vision*. 3836–3847.
- [47] Richard Zhang, Phillip Isola, Alexei A Efros, Eli Shechtman, and Oliver Wang. 2018. The unreasonable effectiveness of deep features as a perceptual metric. In *Proceedings of the IEEE Conference on Computer Vision and Pattern Recognition*. 586–595.
- [48] Xuandong Zhao, Kexun Zhang, Zihao Su, Saastha Vasana, Ilya Grishchenko, C Kruegel, G Vigna, YX Wang, and L Li. 2023. Invisible image watermarks are provably removable using generative ai. *Saastha Vasana, Ilya Grishchenko, Christopher Kruegel, Giovanni Vigna, Yu-Xiang Wang, and Lei Li. "Invisible image watermarks are provably removable using generative ai." Aug (2023).*
- [49] Xuandong Zhao, Kexun Zhang, Yu-Xiang Wang, and Lei Li. 2023. Generative autoencoders as watermark attackers: Analyses of vulnerabilities and threats. *arXiv preprint arXiv:2306.01953* (2023).
- [50] Yunqing Zhao, Tianyu Pang, Chao Du, Xiao Yang, Ngai-Man Cheung, and Min Lin. 2023. A recipe for watermarking diffusion models. *arXiv preprint arXiv:2303.10137* (2023).
- [51] Jiren Zhu, Russell Kaplan, Justin Johnson, and Li Fei-Fei. 2018. Hidden: Hiding data with deep networks. In *Proceedings of the European Conference on Computer Vision*. 657–672.

Received 20 February 2007; revised 12 March 2009; accepted 5 June 2009